Pion double charge exchange on ^{128,130}Te

D. A. Smith, H. T. Fortune, G.-B. Lui,* J. M. O'Donnell,† and M. Burlein‡
University of Pennsylvania, Philadelphia, Pennsylvania 19104

S. Mordechai
Ben-Gurion University of the Negev, Beer-Sheva 84105, Israel
and University of Texas, Austin, Texas 78712

A. R. Fazely
Louisiana State Univeristy, Baton Rouge, Louisiana 70803
(Received 15 October 1991)

Measurements were made of pion double charge exchange on ^{128,130}Te at $\theta_{lab}=5°$ and $T_\pi=292$ MeV. Observations were made of the double isobaric analog, the giant dipole resonance built upon the isobaric analog, and the giant dipole resonance built upon itself. Cross sections for these states were found and compared with all previously known cross sections at $T_\pi=292$ MeV, and new mass dependences were fitted to these data. A new state below the double isobaric analog state in ^{128}Te was observed and its cross section and width were determined.

PACS number(s): 25.80.Gn, 24.30.Cz, 21.10.Hw, 27.60.+j

I. INTRODUCTION

Pion double charge exchange (DCX) is a useful probe to look at resonances and states high in the continuum. States such as the double isobaric analog state (DIAS) will be selectively populated. This state has proven difficult to observe in other reactions [1]. It has been demonstrated in many experiments now that the DIAS is easy to observe using DCX. The DIAS has been populated in many nuclei and the overall mass dependence of the DCX cross section is reasonably understood.

Pion charge exchange has also been shown to be a good way to excite giant resonances high in the continuum, such as the giant dipole resonance (GDR) [2]. The pion is a spin zero particle and, even at resonance energies (100–300 MeV), its small mass serves to keep the total π-nucleus angular momentum low so that pion reactions will favor transitions to states of lower spin in inelastic scattering. This will make the GDR, being a collective 1^- state, stand out against the continuum, and easy to observe. In pion single charge exchange (SCX), the GDR has been seen and measured on many nuclei [2]. In DCX, the GDR has been observed built upon other states, such as built upon the isobaric analog state (GDR·IAS) [3,4] and built upon itself (GDR^2) [5,6]. Although these resonances were first observed only recently, many measurements have now been done on different nuclei, and mass dependences have been determined.

In the present work, cross sections for the DIAS as well as for both giant resonances, the GDR·IAS and the GDR^2 were measured for DCX on ^{128,130}Te at a pion energy of 292 MeV, and a laboratory angle of 5°. The large momentum acceptance of the spectrometer made it possible to see many states in one setting. The values were compared to other data previously published, and new phenomenological mass dependences have been found.

II. EXPERIMENT

The observations were performed using the energetic pion channel and spectrometer (EPICS) at the Clinton P. Anderson Meson Physics Facility (LAMPF) with the standard pion DCX setup [7]. Measurements were taken at the highest energy available, $T_\pi=292$ MeV, and a scattering angle of 5°. The targets used were a 550-mg/cm^2 target of ^{130}Te and a 800-mg/cm^2 target of ^{128}Te, with isotopic purities of 99.46 and 99.39 %, respectively. The targets were made by mixing tellurium metal powder with 9% (by weight) polystyrene and heating under pressure [8]. Data were also obtained in the experiment of pion elastic and double charge exchange on carbon. These were used to subtract the carbon events from the data taken with tellurium targets. Each of the targets was only half the size of the beam so they were put into the beam simultaneously. Figure 1 shows the geometry of the targets in the target frame. Electrons were rejected using a freon-gas velocity-threshold Cherenkov detector in the focal plane. A scintillator placed behind a series of graphite blocks was used to detect and veto muon events. The system was fine tuned by placing aluminum absorbers of variable thickness in front of the first scintillator to ensure that no pions reached the veto scintillator [9]. The remaining background was from pions resulting from DCX to the continuum on the target.

The acceptance of the spectrometer was calibrated from pion inelastic scattering on ^{12}C at a given angle by varying the spectrometer field to cover an outgoing pion momentum range of about ±10% of the central momentum of the spectrometer. Absolute normalizations were obtained from π-p scattering from a polyethylene (CH_2) target of areal density 25.7 mg/cm^2 and comparing the yields with cross sections calculated from π-nucleon phase shifts [10]. The resolution and energy calibration

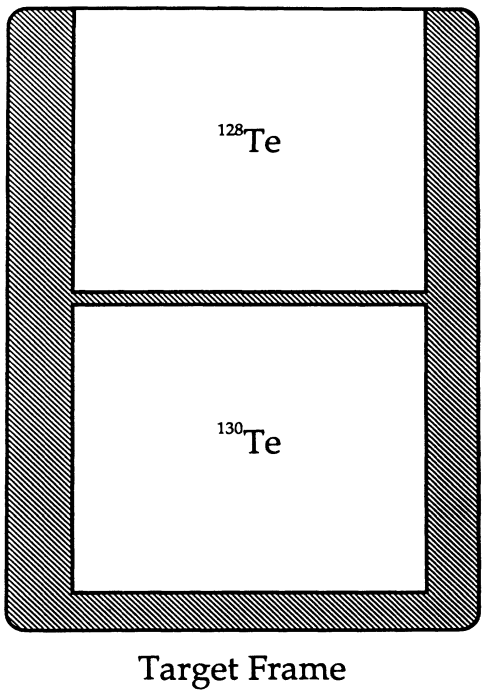

FIG. 1. The geometry of the targets in the target frame when measurements were taken.

of the pion channel were measured from elastic pion data on ^{128,130}Te at the same beam energy and a laboratory angle of 35°.

The choice of the highest beam energy available at EPICS was mainly for the cross sections. Both the DIAS and the GDR have been shown to have cross sections increasing with energy [11,12]. Also, the acceptance of the spectrometer will cover a larger range of outgoing pion energies ($\approx$55 MeV), so both the DIAS and the GDR can be observed. This experiment was aimed primarily at states involving the GDR, but the momentum acceptance of the spectrometer was such that the DIAS could also be seen.

III. RESULTS AND ANALYSIS

Analysis was done to find where the events took place in the target. A histogram of the vertical position of events was made, and target cuts on this histogram differentiated events from ^{128}Te and ^{130}Te. Figure 2 displays the number of events seen as a function of vertical position for tellurium and for hydrogen elastic scattering. For the elastic scattering of pions from hydrogen the histogram just exhibits the shape of the beam and the spectrometer acceptance, but for tellurium there is a clear dip between the two targets. The number of events drops as the position changes from the ^{128}Te target to the thinner ^{130}Te target. Using these cuts, separate spectra of Q values were found for ^{128}Te and ^{130}Te. They are displayed in Fig. 3. These data were then fitted to find cross sections for all states seen. The elastic data on ^{128,130}Te were used to obtain the shape of the reference peak for any state that has no natural width. The DIAS data used this reference peak; the GDR·IAS and the GDR^2 data needed Lorentzians folded with this reference peak shape. The state seen below the DIAS in ^{128}Te was fitted with a Gaussian peak shape folded with the reference peak shape. The background comes from DCX to the continuum and to discrete low-lying states. It is described with a third-degree polynomial. The results of the best fits to these shapes are given in Fig. 4. By comparing the areas of these peaks to that found with the hydrogen normalization runs, cross sections for all states seen in ^{128,130}Te were determined. These cross sections are listed in Table I.

IV. DISCUSSION

Figure 4 displays the ^{128}Te and ^{130}Te (π^+,π^-) Q-value spectra and the fits, showing a narrow state at about -25 MeV, which is the DIAS. The DIAS was fitted with just the reference peak found from elastic scattering, as any Lorentzian folded with this peak produced a natural width of zero for the DIAS. Cross sections were determined for this peak and can now be compared to all other cross sections for DCX to the DIAS at T_π=292 MeV at 5°. Johnson suggested that the mass dependence of the DIAS should be [13]

$$\frac{d\sigma}{d\Omega}(q=0) \propto (N-Z)(N-Z-1)A^{-10/3} .$$

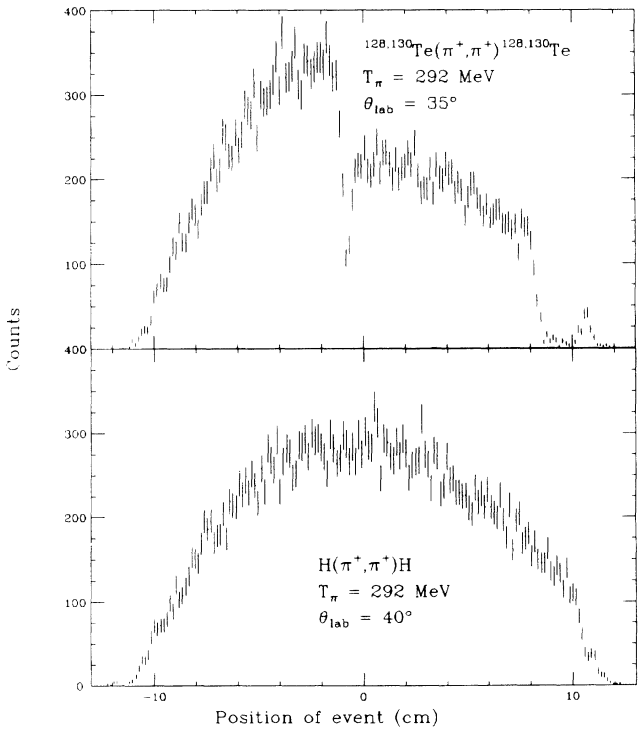

FIG. 2. Histograms showing vertical positions of events on the target. The hydrogen elastic measurements were done with a full target, and the histogram shows the shape of the beam. The tellurium elastic data show the differences between the two targets in the beam, the thicker ^{128}Te target being on the left. The small peak on the far right is the edge of the target frame.

TABLE I. Cross sections found in this work for (π^+,π^-) at $T_\pi=292$ and $\theta_{lab}=5°$.

Target	State	$-Q$ (MeV)	Width (MeV)	$d\sigma/d\Omega$ (μb/sr)
^{128}Te	State 1	16.64±0.24	0.74±1.04	0.15±0.05
	DIAS	25.78±0.05		0.73±0.10
	GDR·IAS	36.19±0.52	3.87±0.95	1.75±0.37
	GDR^2	44.56±1.06	10.4±1.90	5.78±0.80
^{130}Te	DIAS	25.49±0.08		0.76±0.16
	GDR·IAS	36.40±0.05	4.48±1.83	2.31±0.44
	GDR^2	47.31±0.63	8.40±1.98	8.03±1.97

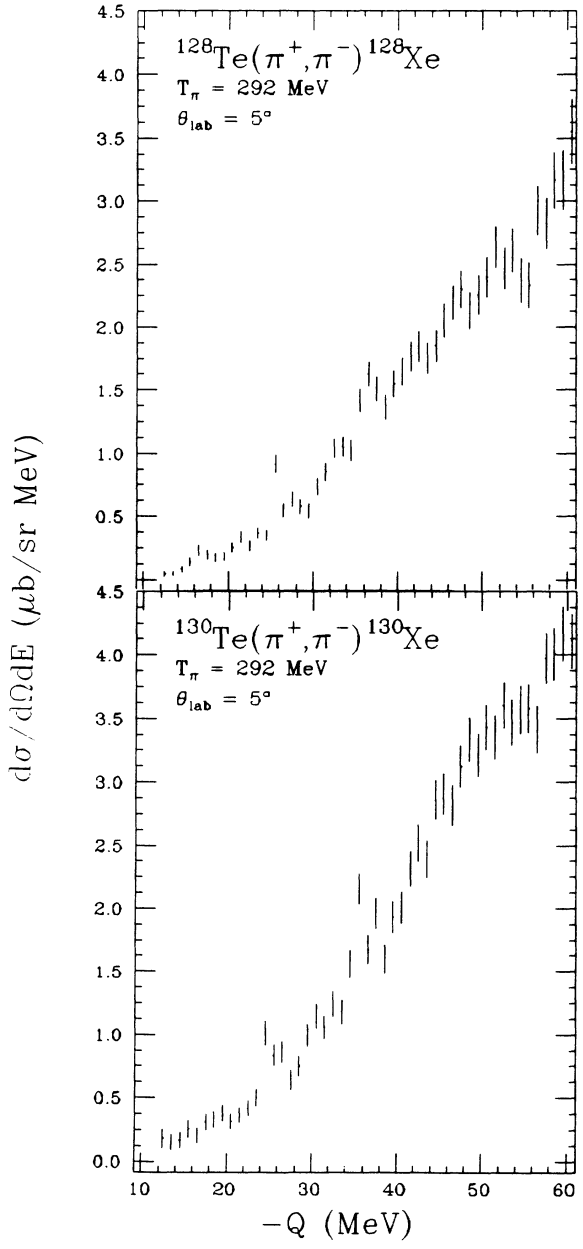

FIG. 3. Data measured in this work. The points are shown in 1-MeV bin size.

The $(N-Z)$ factor is for single charge exchange to the IAS, and the $(N-Z-1)$ factor is for the second charge exchange to the DIAS. Fits to the available data at the time seemed to suggest that this formula was valid [14]. Later, as more DIAS cross sections became available, it was noted that this formula is insufficient. In particular, $T=1$ nuclei exhibit a mass dependence of $A^{-7/3}$ for the DIAS data [15]. It appeared that this effect was just for the $T=1$ nuclei, and that other DIAS data could still be fitted with $A^{-10/3}$. All DIAS data that are now available have been fitted using just the $A^{-10/3}$ function, and by

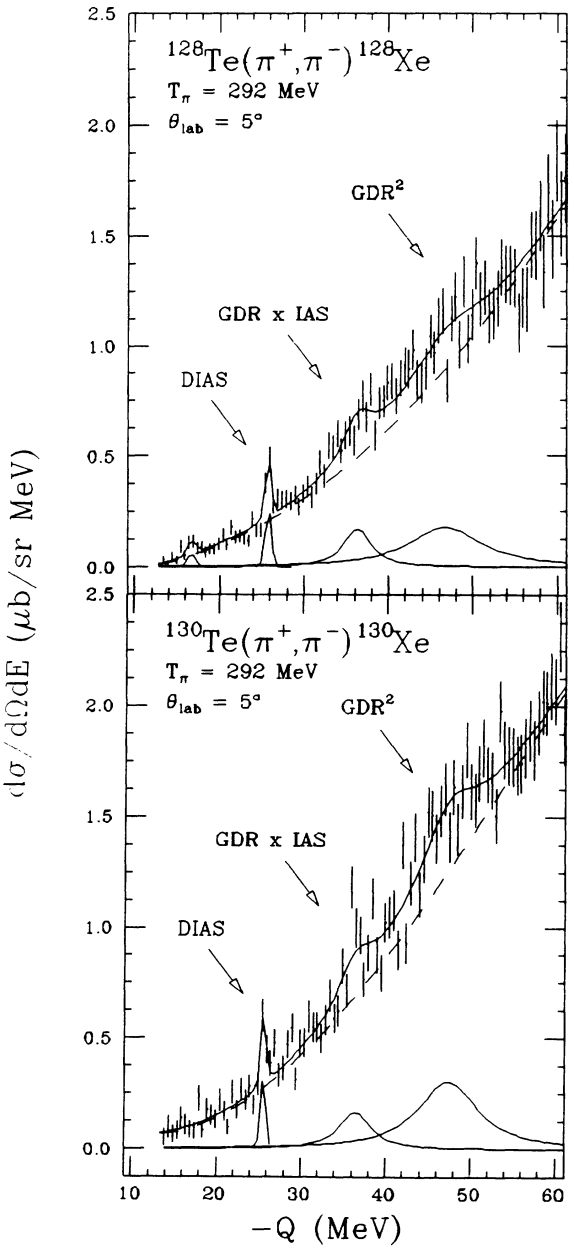

FIG. 4. Data as measured in this work and the fittings used to find the cross sections for the various states. The DIAS is fitted with the peak shape measured from elastic scattering, the giant resonances are fitted with Lorentzians folded with this peak shape. The background is a third-degree polynomial.

TABLE II. Fittings used for the DIAS. All formulas are fitted by $[d\sigma/d\Omega(5°)]/(N-Z)(N-Z-1)$.

Scaled σ fit	f (μb/sr)	χ^2
$f(A^{-10/3})$	17710±417	4.47
$f(A^{-7/3})$ for $T=1$	988±38.5	
$f(A^{-10/3})$ for $T\neq 1$	17728±514	2.86
$f(A^{-7/3})$ for $T=1$	988±38.5	
$f(A^{-7/3})$ for $44\leq A\leq 93$	231±7.1	
$f(A^{-7/3})$ for $128\leq A\leq 209$	104±9.6	2.10

using $A^{-7/3}$ for $T=1$ nuclei and an $A^{-10/3}$ curve for the rest. The results of this fitting are shown in Table II. By looking at the reduced χ^2, the mixed dependence fit is the better one, but it is still not satisfactory. The $A^{-10/3}$ dependence comes just from geometry arguments, but if a microscopic calculation is done, a mass dependence closer to $A^{-7/3}$ is found [16]. But using an $A^{-7/3}$ mass dependence over the full range of data does not produce a good fit. However, if three different multiplicative factors exist for different A ranges in the fit, the $A^{-7/3}$ dependence looks better. The results from a three-step fit are also given in Table II. The reduced χ^2 of this fit suggests that it is still not the best fit, but it is better than the other two. Figure 5 contains all the DIAS data [7,14-25] and the $A^{-10/3}$ fit compared to the three-step fit. The origin of this stair-step mass dependence is not known, as theory does not predict it.

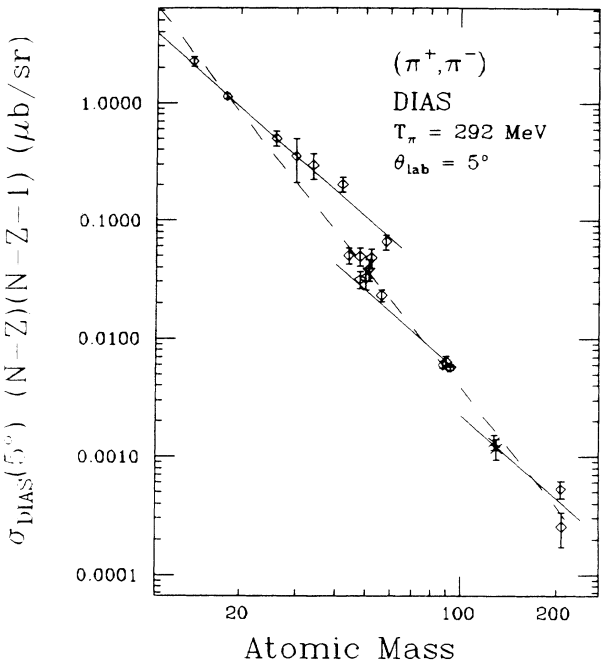

FIG. 5. All published values for the DIAS cross sections at $\theta_{lab}=5°$ and $T_\pi=292$ MeV. The dashed curve is the best fit $A^{-10/3}$ for all data $T\neq 1$. The solid curves are the best fit $A^{-7/3}$ for $T=1$, $44\leq A\leq 93$, and $128\leq A\leq 209$ data, parameters are given in Table II.

Higher in the continuum is the giant resonance built upon the isobaric analog state (GDR·IAS). It comes about as a collective dipole operator acting upon the isobaric analog state [3,4]. This state has been seen in many nuclei and is a general feature of all nuclei with $N-Z\geq 1$ [4]. The mass dependence of the GDR·IAS has been worked out to be of the form

$$\frac{d\sigma}{d\Omega}(\text{peak})\propto(N-Z)(NZ)A^{-x}\ .$$

The $(N-Z)$ factor is for single charge exchange to the IAS, and the (NZ) factor is for the giant resonance. But this formula is expected to work best for the peak cross-section values. The GDR·IAS is a 1^- state, and will not have its peak value at 5° where the tellurium data were measured. A distorted-wave calculation was performed for DCX on tellurium, using a coupled-channels code called NEWCHOP [26]. In the calculations, the GDR·IAS angular distribution peaks at 10°. The strengths for the coupled-channels calculations were fitted to the 5° datum and used to determine the 10° peak cross section. These cross sections are listed in Table III. These values along with all other peak values published for DCX to the GDR·IAS were then fitted with the above form of the mass dependence [3,4,27]. The results of this fit with just

TABLE III. Fittings used for the GDR·IAS data. All formulas are fitted by $[d\sigma/d\Omega(\text{peak})]/(NZ)(N-Z)$.

Scaled σ fit	A_0	f (nb/sr)	x	χ^2
$f(A/A_0)^{-x}$	59	0.371±0.015	2.461±0.048	6.16
$f(A/A_0)^{-x}$ for $T=\frac{1}{2}$	27	3.242±0.330	1.710±0.211	
$f(A/A_0)^{-x}$ for $T\neq\frac{1}{2}$	93	0.121±0.006	2.605±0.097	5.18
$f(A/A_0)^{-x}$ for $T=\frac{1}{2}$	27	3.242±0.330	1.710±0.211	
$f(A/A_0)^{-x}$ for $56\leq A\leq 80$	59	0.443±0.031	2.072±0.765	
$f(A/A_0)^{-x}$ for $93\leq A\leq 208$	130	0.042±0.003	1.526±0.228	0.80
$f(A^{-5/3})$ for $T=\frac{1}{2}$		798.5±61.1		
$f(A^{-5/3})$ for $56\leq A\leq 80$		387.8±26.6		
$f(A^{-5/3})$ for $93\leq A\leq 208$		138.0±8.69		0.75

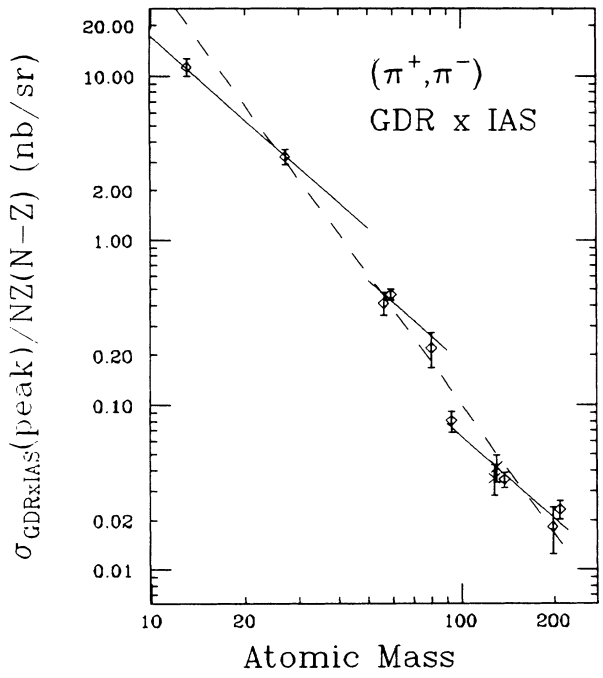

FIG. 6. All published data for the GDR·IAS peak cross-section values for $T_\pi = 292$ MeV. The dashed curve is the best-fit power law for all $T \neq \frac{1}{2}$ data. The solid curves are $A^{-5/3}$ for $T = \frac{1}{2}$, $56 \leq A \leq 80$, and $93 \leq A \leq 208$ data, with parameters in Table III.

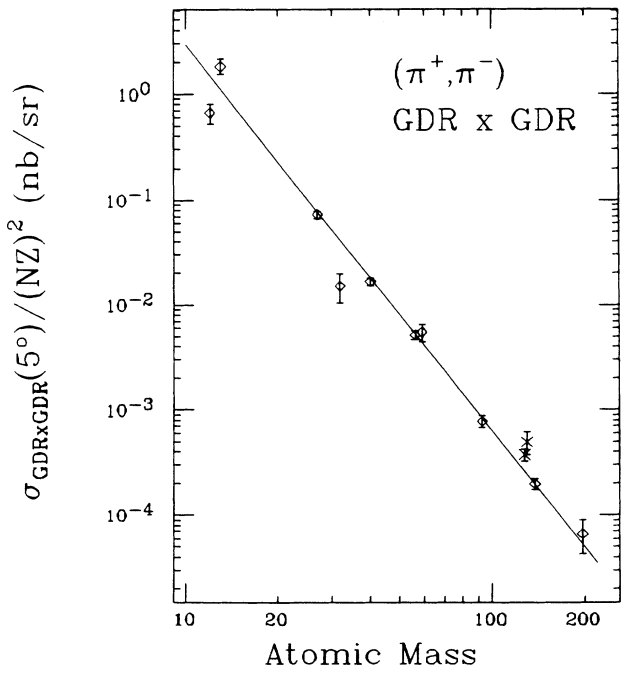

FIG. 7. All published data for the GDR^2 cross sections at $\theta_{lab} = 5°$ and $T_\pi = 292$ MeV. The solid line is the best-fit $A^{-11/3}$ curve, listed in Table IV.

TABLE IV. Fittings used for the GDR^2 data, except for ^{12}C, ^{32}S. All formulas are fitted by $[d\sigma/d\Omega(5°)]/(NZ)^2$.

Scaled σ fit	A_0	f	x	χ^2
$f(A/A_0)^{-x}$	59	$(4.60\pm0.18)\times10^{-3}$ nb/sr	3.62 ± 0.06	2.38
$f(A^{-11/3})$		13.56 ± 0.54 μb/sr		2.05

a single power of A are given in Table III. The χ^2 suggests it to be bad fit. As this state involves the IAS (just as the DIAS does), the fact that the DIAS has a different mass dependence for $T = 1$ nuclei might imply that this state should have a different mass dependence for $T = \frac{1}{2}$

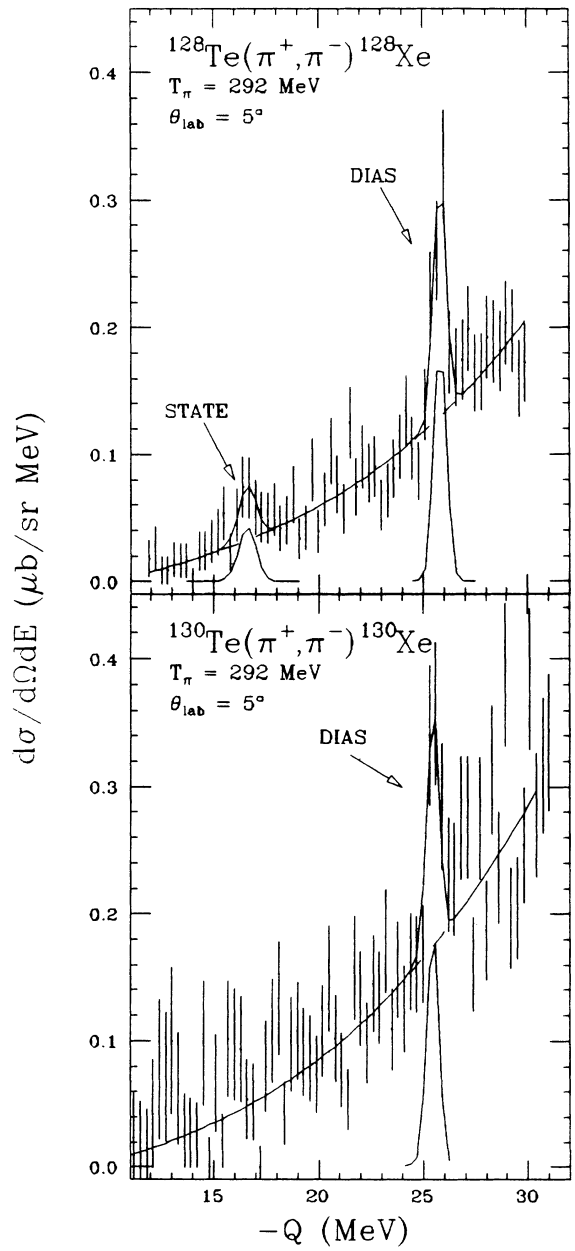

FIG. 8. Low Q-value data measured in this work. The ^{128}Te spectrum shows a weakly excited state below the DIAS in excitation. The ^{130}Te spectrum shows no such state.

nuclei. Isospin considerations also reduce the cross sections for the $T=\frac{1}{2}$ targets. The given data were than fitted at two different mass dependences, one power for $T=\frac{1}{2}$ nuclei and a different multiplicative constant and power law for the rest of the data. This gives a better fit. However, all states built on the IAS may have a related mass dependence, so that the GDR·IAS data might exhibit the same three-step dependence as the DIAS. A three-step mass dependence was tried with individual power laws for each step (Fig. 6). The mass ranges for each step are the same as the ones used for the DIAS mass dependence, except for ^{93}Nb. Niobium is on the edge of having a closed neutron shell, so the strength populating the IAS may be very different than for the DIAS. The results of the two and three dependence fits are given in Table III. The three-step dependence is a remarkably better fit. The powers for the three steps are all consistent with $-\frac{5}{3}$ and the average of the three also gives a power of $-\frac{5}{3}$. A fit with just this power for the three steps was performed, and the results are also listed in Table III, the χ^2 shown are reduced. With just the assumption of an $A^{-5/3}$ power law and given three steps, the data are well fitted. It is remarkable that such a simple mass dependence fits these data so well.

Still higher in the continuum is found the giant dipole resonance built upon itself (GDR^2). This resonance has been seen in many nuclei and is accepted as a general feature of all nuclei [6]. In all nuclei, the Q value of this state has been observed to be around -50 MeV, and the tellurium data are consistent with these previous observations. The widths of the GDR^2 in all nuclei are around 9 MeV, and these observations are also consistent with the tellurium data.

A general mass dependence for the GDR^2 in all nuclei has been assumed to be

$$\frac{d\sigma}{d\Omega}(5^\circ) \propto (NZ)^2 A^{-x} .$$

Each GDR step provides an (NZ) factor for the giant resonance. All published data for the GDR^2 at $T_\pi=292$ and 5° have been compiled and fitted with just the above mass dependence [5,6,28]. Only two points lie more than three sigma away from any simple fitting, and these are for ^{32}S and ^{12}C. These points were removed and a single power law was then found to provide an adequate description. The exponent is consistent with $-\frac{11}{3}$, and the data were then fitted with a mass dependence power law of $-\frac{11}{3}$. The results of these fits are given in Table IV, and the data and the power-law fit are displayed in Fig. 7, the χ^2 shown are reduced. This result suggests that the GDR^2 has a very simple mass dependence with few exceptions. The three-step dependence exhibited by the states built upon the IAS probably comes from shell effects on the IAS cross sections.

Along with the DIAS, GDR·IAS, and GDR^2, in ^{128}Te there was found one other state. This state is weaker than the ones discussed and lies below the DIAS in excitation. In Fig. 8 an enlargement of the low-energy part of the Q-value spectrum is shown with the fits. The DIAS is the main peak, and below the DIAS in ^{128}Te is a weakly excited state. The spectrum for ^{130}Te does not exhibit any states of this kind. This state does have some measurable width and is probably two single states lying close together which cannot be separated given the resolution of these measurements. The nature of this state is unclear at this time.

V. CONCLUSION

Pion DCX on these two isotopes of tellurium possesses the major features that have been seen in previous DCX measurements. The addition of these data has given a new mass dependence for all known collective states in DCX. The DIAS now has a mass dependence of $A^{-7/3}$, the GDR·IAS $A^{-5/3}$ and the GDR^2 $A^{-11/3}$. These numbers are not easy to understand given that the power from the GDR·IAS should lie between that for the DIAS and the GDR^2. Also, a stair-step dependence has been found for states built upon the IAS. The cause has yet to be determined. A new state has been seen in ^{128}Te lying in excitation below the DIAS.

This work was supported by grants from the National Science Foundation and the U.S. Department of Energy.

*Present address: Department of Medical Physics, Memorial Sloan-Kettering Cancer Center, 1275 York Ave. SM08, New York, NY 10021.

†Present address: Los Alamos National Laboratory, Mail Stop H841, Los Alamos, NM 87545.

‡Present address: Operational Evaluation Divisoin, Institute for Defensive Analysis, 1801 N. Beauregard St., Alexandria, VA 22311.

[1] G. W. Hoffman, G. J. Igo, C. A. Whitten, Jr., W. H. Dunlop, and J. G. Kulleck, Phys. Rev. Lett. **28**, 41 (1972).

[2] A. Erell, J. Alster, J. Lichtenstadt, M. A. Moinester, J. D. Bowman, M. D. Cooper, F. Irom, H. S. Matis, E. Piasetzky, and U. Sennhauser, Phys. Rev. C **34**, 1822 (1986).

[3] S. Mordechai *et al.*, Phys. Rev. Lett. **60**, 408 (1988).

[4] S. Mordechai *et al.*, Phys. Rev. C **40**, 850 (1989).

[5] S. Mordechai *et al.*, Phys. Rev. Lett. **61**, 531 (1988).

[6] S. Mordechai, S. Mordechai, H. T. Fortune, J. M. O'Donnell, G. Lui, M. Burlein, A. H. Wuosmaa, S. Greene, C. L. Morris, N. Auerbach, S. H. Yoo, and C. F. Moore, Phys. Rev. C **41**, 202 (1990).

[7] S. Green, Ph.D. thesis, University of Texas (Los Alamos Report LA-8891-T), 1981.

[8] A. Fazely *et al.*, Phys. Lett. B **208**, 361 (1988).

[9] C. L. Morris, J. F. Amann, R. L. Boudrie, N. Tanaka, S. J. Seestrom-Morris, L. C. Bland, P. A. Seidl, R. Kiziah, and S. J. Greene, Nucl. Instrum. Methods A **238**, 94 (1985).

[10] G. Rowe, M. Salomon, and R. H. Landau, Phys. Rev. C **18**, 584 (1978).

[11] A. Williams *et al.*, Phys. Rev. C **43**, 766 (1991).

[12] F. Irom *et al.*, Phys. Rev. C **34**, 2231 (1986).
[13] M. B. Johnson, Phys. Rev. C **22**, 192 (1980).
[14] C. L. Morris *et al.*, Phys. Rev. Lett. **45**, 1233 (1980).
[15] P. Seidl *et al.*, Phys. Rev. C **30**, 973 (1984).
[16] R. Gilman *et al.*, Phys. Rev. C **35**, 1334 (1987).
[17] J. Zumbro *et al.*, Phys. Rev. C **36**, 1479 (1987).
[18] R. Gilman, H. T. Fortune, J. D. Zumbro, P. A. Seidl, C. F. Moore, C. L. Mooris, J. A. Faucett, G. R. Burleson, S. Mordechai, and K. S. Dhuga, Phys. Rev. C **33**, 1082 (1986).
[19] M. Kaletka, K. K. Seth, A. Saha, D. Barlow, and D. Kielczewska, Phys. Lett. B **199**, 336 (1987).
[20] P. Seidl *et al.*, Phys. Rev. Lett. **50**, 1106 (1983).
[21] P. Seidl *et al.*, Phys. Rev. C **42**, 1929 (1990).
[22] K. K. Seth, M. Kaletka, D. Barlow, D. Kielczewska, A. Saha, L. Casey, D. Godman, R. Seth, and J. Stuart, Phys. Lett. **155B**, 339 (1985).
[23] C. L. Morris *et al.*, Phys. Rev. Lett. **54**, 775 (1985).
[24] S. J. Greene *et al.*, Phys. Rev. C **25**, 927 (1982).
[25] K. K. Seth, S. Iversen, M. Kaletka, D. Barlow, A. Saha, and R. Soundranayagan, Phys. Lett. B **173**, 397 (1986).
[26] E. Roset, computer code CHOPIN (unpublished). The code has been modified by C. L. Morris to calculate pion charge exchange reaction and renamed NEWCHOP.
[27] S. Mordechai *et al.*, Phys. Rev. C **43**, 1111 (1991).
[28] S. Mordechai *et al.*, Phys. Rev. C **43**, R1509 (1991).